Conference on
Applied Motion Control 1987

ALTERNATIVE MODELING AND VERIFICATION TECHNIQUES FOR A LARGE FLEXIBLE ARM

James D. Huggins
Dong-Soo Kwon
Jae Weon Lee
Dr. Wayne J. Book

George W. Woodruff School of Mechanical Engineering
Georgia Institute of Technology
Atlanta, Georgia 30332

I. INTRODUCTION

Traditional robot manipulators have been designed for rigidity with short arm lengths and heavy steel construction in order to achieve positional accuracy and stability of the robot's movements. An alternative approach is to use lightweight materials for construction of the manipulator and to design the structure based primarily on strength requirements. This approach leads to flexible structures in which the flexible motion of the manipulator itself must be controlled either by control algorithms or by passive damping.

Lightweight manipulators have a number of advantages over rigid manipulators. These include low power consumption, high load to weight ratios, large workspaces, and the potential for high speed operation because of lower inertia. In addition, lightweight robots can be more easily designed as self-contained, fully mobile units or as semi-permanent units that can be easily transported.

A large two degree of freedom flexible manipulator has been constructed at Georgia Institute of Technology [1] for research purposes. The structure consists of two ten foot long links made of aluminum tubing actuated by hydraulic cylinders. This large size was chosen to realistically represent a flexible manipulator in a region of design space where it would be most competitive, since small manipulators can be more easily and economically built to be nearly rigid.

For modeling this structure, two methods have been used. The first model is the non-linear "assumed modes" model. It represents link deflections using assumed mode shapes. The manipulator links are modeled as Bernoulli-Euler beams and the vibration modes are approximated by a finite number of mode shapes. Using this method, the compact closed form equations for general (large, high speed) motion are derived by a symbolic manipulation software package. [2] Unlike the single link case, the derivation of the mode shapes of a multi-link manipulator is very difficult using this analytical method since exact boundary conditions are hard to determine and depend on the configuration of the manipulator and its control algorithm. The flexible closed loop chain involved in actuating the second link sets this modeling effort apart from other efforts in the robotics or mechanism literature.

Second, the flexible manipulator is modeled using a finite element method. [3] The advantage of the finite element method is that it provides a systematic way for modeling complex geometries with linear small motion dynamics. However, it is unsuitable for simulation because the computations require too much time. This paper presents comparisons made between the experimentally determined system mode shapes and natural frequencies and the corresponding values obtained from the finite element analysis and the eigenvectors and eigenvalues of the linearized assumed mode method.

II. DESCRIPTION OF MODELING METHODS

ASSUMED MODES METHOD

System description

The schematic drawing of this manipulator is shown in Fig. 1. The structure consists of two 10 foot long links made of aluminum tubing. The lower link is driven by a hydraulic actuator and the upper link is driven by a parallel link mechanism using a hydraulic actuator. The actuating link is made from rectangular aluminum tubing. This system is assumed to have vertical plane motion . To simplify the analysis, the cylindrical sleeves at the connection of the lower link and the upper link are modeled as concentrated masses. Other sleeves on the lower link are neglected. The dynamics of the hydraulic actuators are also neglected.

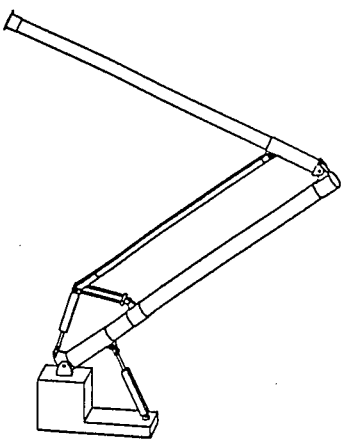

Flexible Manipulator at Georgia Tech
Fig. 1

Equations of motion

For modeling of a manipulator having a closed chain, the topological open tree with unknown constraint force between the actuating link and the upper link is constructed by cutting the joint. The dynamics of the open tree structure can be formulated easily via Lagrange's equation. In order to describe the motion, the reference frame should be defined as shown in Fig 2. The absolute position vectors of an arbitrary point on each link are described by two sets of generalized coordinates, rigid and elastic.

$$\bar{r}_i = \bar{R}_i + \bar{U}_{r_i} + \bar{U}_{f_i} \qquad (2.1)$$

where $\bar{R}_i$ is the position vector of the origin of the reference body measured with respect to the global frame, U_{ri} is the undeformed position of each link, and U_{fi} is the elastic deflection vector, which is composed of a linear combination of an admissible shape function, Φ, multiplied by time dependant elastic coordinates:

$$\bar{U}_{f_i}(x,t) = \sum_{j=1}^{n} \Phi_{ij}(x)\, q_{f_{ij}}(t) \qquad (2.2)$$

Assuming that the amplitude of the higher modes of flexible links is very small compared with the first assumed mode, the system can be truncated with n equal to 2.

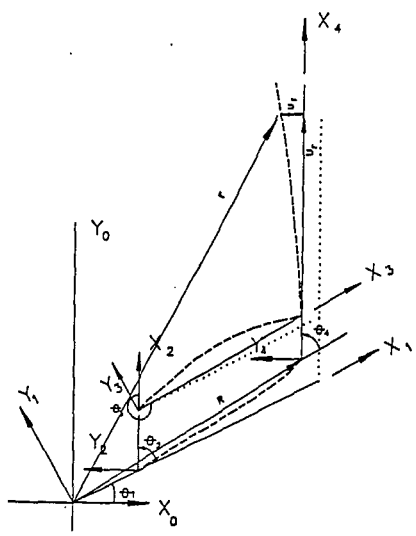

Coordinate Systems of Assumed Modes Model
Fig. 2

The kinetic energy, T_i, of each element is obtained from the velocity vector of the infinitesimal volume:

$$T_i = \frac{1}{2} \rho \int \dot{\bar{r}}_i \cdot \dot{\bar{r}}_i dV \qquad (2.3)$$

The potential energy, V_i, of each element is composed of the strain energy (since gravity is a static term, it is not considered). The strain energy, which is stored in the flexible mode, can be attributed to the elastic stiffness, K_i, which is evaluated by integration over the length of the beam:

$$K_i = (EI)_i \int \Phi_{ij}''^{\,2}\, dx \qquad (2.4)$$

$$V_i = \frac{1}{2} q_i^T K_i q_i \qquad (2.5)$$

where E is Young's modulus of elasticity, and I is the area moment of inertia.

The governing dynamic equations for the system are derived through Lagrange's equations:

$$\frac{d}{dt}\left(\frac{\partial T}{\partial \dot{q}_j}\right) - \frac{dT}{dq_j} + \frac{dV}{dq_j} = Q_e \qquad (2.6)$$

The algeraic complexity in applying Lagrange's equation can be overcome by using a symbolic manipulation program. The resulting dynamic equations are a coupled set of second order equations:

$$[M]\,\ddot{q} + [K]\,q = Q \qquad (2.7)$$

where Q includes the external force, Q_e, plus the quadratic velocity terms resulting from differentiating the kinetic energy with respect to time and with respect to the generalized coordinates. The motion of the open tree system is constrained by a set of nonlinear algebraic constraint equations.

$$\Phi(q) = 0 \qquad (2.8)$$

These constraint relations can be adjoined to equation (2.6) using Lagrange multipliers so that:

$$[M]\,\ddot{q} + [K]\,q = Q + \Phi_q^T \lambda \qquad (2.9)$$

where Φ_q^T is the constraint Jacobian matrix and λ is the vector of Lagrange multipliers. This equation can be written in partitioned form in terms of the rigid and elastic coordinates as:

$$\begin{bmatrix} M_{rr} & M_{rf} \\ M_{fr} & M_{ff} \end{bmatrix} \begin{Bmatrix} \ddot{q}_r \\ \ddot{q}_f \end{Bmatrix} + \begin{bmatrix} 0 & 0 \\ 0 & K_{ff} \end{bmatrix} \begin{Bmatrix} q_r \\ q_f \end{Bmatrix} = \begin{bmatrix} Q_r \\ Q_f \end{bmatrix} + \begin{bmatrix} \Phi_{qr} \\ \Phi_{qf} \end{bmatrix}^T \lambda \qquad (2.10)$$

In order to find the natural frequencies and mode shapes with the measured data, only the vibration of the flexible body relative the rigid body is considered. The system equations of motion can then be written as:

$$[M_{ff}]\,\ddot{q}_f + [K_{ff}]\,q_f = Q_f + \Phi_{q_f}^T \lambda \qquad (2.11)$$

Free vibration, where external forces and constraint forces become zero, yields: [4]

$$[M_{ff}]\ddot{q}_f + [K_{ff}]q_f = 0 \qquad (2.12)$$

This equation represents a set of homogeneous equations whose nontrivial solution defines a finite number of eigenvalues and their associated eigenvectors. The eigenvalues define the system natural frequencies and the eigenvectors determine a relative magnitude of each mode shape.

For numerical analysis, selection of shape functions is necessary and may greatly influence the results. Clamped-mass boundary conditions are assumed for the lower link mode shape. The mode shape equation is: [5]

$$\Phi_{1i} = \cos(\frac{\lambda_{1i}x}{L}) - \cosh(\frac{\lambda_{1i}x}{L}) + \sigma_{1i}\{\sinh(\frac{\lambda_{1i}x}{L}) - \sin(\frac{\lambda_{1i}x}{L})\} \qquad (2.13)$$

The mode shape equation for the upper beam using clamped-free boundary conditions is: [6]

$$\Phi_{3i} = \cosh(\frac{\lambda_{3i}x}{L}) - \cos(\frac{\lambda_{3i}x}{L}) - \sigma_{3i}\{\sinh(\frac{\lambda_{3i}x}{L}) - \sin(\frac{\lambda_{3i}x}{L})\} \qquad (2.14)$$

and the mode shape equation for the actuating link using pin-pin boundary conditions is:

$$\Phi_{2i} = \sin(\frac{i\pi x}{L}) \qquad (2.15)$$

FINITE ELEMENT METHOD

The finite element method is a very useful method especially when it is necessary to reconcile the discrepancies between the theoretical model and the real system due to the theoretical model's simplification. Since the parameters of the theoretical model can be easily changed to reflect various degrees of model reduction, several sets of parameters can be used in order to determine the amount of simplification necessary. In a complex multi-link system, the exact boundary conditions are unknown, so that there is no basis for assuming any mode shapes for the links. The finite element model provides a method of choosing the proper boundary conditions because the dominant mode shapes of each link can be found from analysis of the system modes.

In this dynamic analysis, the large flexible manipulator was modeled using linear isotropic three dimensional beam elements and lumped mass elements. Therefore, the model allows flexural and axial vibrations in all three axes directions. For boundary conditions, the ends of the hydraulic actuators were fixed to the ground by pin joints, so that these joints have zero translational displacements and allow only z axis rotation. See Fig. 3. All beams and links are connected with pin joints using idealized coupled constraints. To describe the pin joints, the coupled constraint condition allows only one rotational degree-of-freedom about the z-axis between the coupled nodes at the joints. [3] When only two dimensional motion was analyzed, the z-axis translational degree-of-freedom and the x and y axes rotational degrees-of-freedom were restricted by nodal displacement restraints. [3] The hydraulic actuators were modeled as rigid links. The coulomb friction at the joints and the structural damping of the beams were ignored in the dynamic analysis.

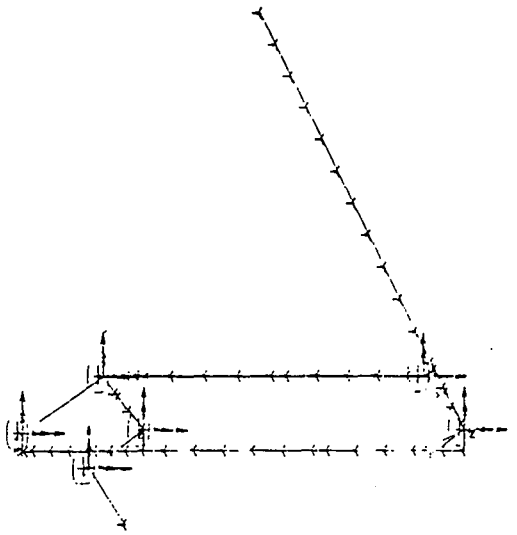

Nodes of Finite Element Model
Fig. 3

Two types of finite element models were created: one is a simplified model with seven kinds of beam elements and one lumped mass element using the same physical dimension data and rigidity assumptions as the assumed modes model, the other model uses more detailed dimensional data, thirteen kinds of beam elements and three kinds of lumped mass elements so that it more closely matches the actual structure. The second model makes no assumptions about the rigidity of any of the links. Only the hydraulic actuators are assumed rigid. These two models can be used to explain the discrepancy between the assumed mode method and the results of the experiment. For dynamic analysis, the simultaneous vector iteration method was used to obtain the natural frequencies and system mode shapes. [12]

DESCRIPTION OF EXPERIMENT

The arm built for this and other research in lightweight robots consists of two ten foot long links moving in a vertical plane. The two links are constructed from four and five inch diameter aluminum pipe, wall thickness - .12 and .134 inches, respectively. The third member, the actuator link, is made from 1.75 x 4.0 inch rectangular aluminum tubing. Eighteen inch long cylindrical sleeves are used to connect the joints of the structure to the

links. The moving structure (links and joints) weigh approximately 70 lbs. The axes of the joints are parallel and are made using steel pins inside bronze bushings. Any motion outside of the vertical plane is caused by structural asymmetries. Hydraulic cylinders provide the motive power for the manipulator. As can be seen from Figure 1., both actuators are located near the base of the manipulator. The upper link is actuated through the use of a parallel four bar linkage. This was done to reduce the inertia of the structure while supplementing its rigidity, but it tends to increase the complexity. Refer to Fig. 4 for the nomenclature of the structure.

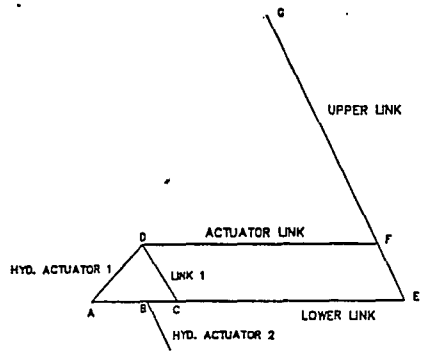

Nonmenclature of Structure
Fig. 4

One of the most practical comparisons to make between a dynamic system and its model is the linear behavior for small motions about an operating point. For vibrational systems with light damping, this is equivalent to comparisons of the natural frequencies, damping ratios, and system mode shapes. Since the assumed mode shape model results in a drastic reduction in order from either the real system or the finite element model, verification of this type of model is especially important. While analytical methods, such as a balanced realization have been applied to choosing the model order, [7] such techniques assume the high order model to be perfect. For reasonably complex and imperfect structures, such as discussed here, experiments are an essential part of developing a believable model. For the flexible and non-linear assumed modes model, this paper only addresses verification of the flexible aspects, not the non-linear aspects.

Several different methods [8] were tried to accurately measure the modal properties of the manipulator. Among these were step relaxation and impact hammer methods, exciting the structure with the an electromagnetic shaker, and exciting the structure with the hydraulic actuators themselves. Of these, the electromagnetic shaker was chosen to excite the structure because of its ability to excite the higher frequencies, our ability to gather phase information as well as frequency information, and because of its accuracy and ease of implementation. Additionally, several types of input signals were compared. [9] These included random noise, burst random noise, swept sine, and periodic burst chirp. All input sources yielded the same frequency characteristics for this structure. Random noise became the input of choice because of its ease of use and because there tended to be slightly less noise in the measurements. All measurements were made using the same input amplitude. Piezoelectric transducers were used to measure the input force and the acceleration at various measurement points on the structure. The signals from these transducers were used as inputs into a two channel digital signal analyzer.

Two different configurations of the structure were experimentally analyzed for resonant frequencies and for mode shapes. It was soon found that the configuration had a small effect on the natural frequencies and mode shapes. This was particularly true of the higher frequencies. For this reason, only the data from one of the configurations is presented here.

To measure the mode shapes of the manipulator, each link was marked in 6 inch increments. The accelerometer was mounted at the marked positions in the plane of links and perpendicular to the links. The structure was then excited with the electromechanical shaker and 30 averages of the frequency response were taken to minimize noise effects. The frequency response measurements were calculated using the cross spectrum function. [10] This method provides both magnitude and phase information. The correlation of the two signals was also checked at each measurement point.

To measure the effect of using hydraulic cylinders as actuators, a turnbuckle was installed in place of the lower cylinder. Measurements of the accelerations of the structure were then made. The hydraulic cylinder was reinstalled and acceleration measurements were made at the same points. using various hydraulic pressures to determine the effect of compressibility of the hydraulic fluid. No appreciable difference in the frequency response of the structure was noticed even though the pressure was increased by a factor of three. Also, a turnbuckle was used in place of the hydraulic actuator for the upper link in order to eliminate any hydraulic effects of that actuator.

Displacement of the structure is calculated by first displaying the imaginary part of the frequency response, then using "artificial integration," [11] ie. dividing by $j\omega$, to obtain a relative value of displacement. This technique also provides information about the phase of the mode shapes. The true value of the magnitude due to vibration is a function of the input torque. The structural damping was determined with a built-in function of the digital signal analyzer. The values of the damping ranged from .005 at 54.37 Hz to .014 at 6.37 Hz. The natural frequency determinations and the respective mode shapes determined from each of the three methods are presented in the next section.

III. RESULTS

As can be seen from Table 1., there is not perfect agreement between the three methods used to analyze this flexible structure.

System Modes	Assumed Modes Method	F.E. Method 1	F.E. Method 2	Experimental Method
1	6.40	7.80	5.95	6.37
2	17.00	15.90	12.78	12.00
3	30.00	30.80	30.19	37.87
4	**	**	60.60	54.37
5	93.60	94.69	95.95	92.00

** Not Predicted 1 - Simplified Model
2 - Detailed Model

System Modes, Experimental and Theoretical
Table 1.

Several explanations can be offered for the discrepancies:

1. Both the assumed mode method and the finite element method assume that the structure has ideal characteristics. That is, that the pin joints have no friction, that there is no mechanical looseness in the structure, that the actuators are rigid, that the base is rigid, that every joint is perfectly parallel, and that there is no structural damping.
2. The finite element software assumes that the structure is linear and the assumed modes method uses a linearized version of the non-linear model.
3. It is very difficult to model the actual structure geometry using the Bernoulli-Euler techniques.
4. The boundary conditions (clamped-mass, pin-pin, clamped-free) used in theoretical results cannot be precisely duplicated in a less than ideal structure.

As can be seen in Fig. 5a, the first system mode, at 6.37 Hz, is dominated by the first bending mode of the lower link. By using clamped-mass boundary conditions, both analytical methods accurately predict this natural frequency and mode shape. The second system mode is dominated by the first bending mode of the upper link as seen in Fig. 5b. Using clamped-free boundary conditions in the assumed modes model and using the simplified finite element model, there was a 4 Hz discrepancy with the experimental results. When the lower link's geometry was modeled more accurately in the detailed finite element model, there was much better agreement of this method with the experimental results. It is seen, then, that the simplified F.E. model agrees well with the assumed modes model and that the detailed F.E. model agrees well with the experimental results.

The largest discrepancy between the experimentally determined and the theoretically predicted natural frequencies occurs in the third and fourth system modes. The third system mode is dominated by the pin-pin bending mode of the actuator link, but unlike the first two modes, there is nearly a 7 Hz discrepancy between the measured and predicted natural frequencies. However, as can be seen in Fig. 5c, the mode shapes from all three methods correspond well. The explanation for this is that the third mode primarily involves the vibration of the actuator link. Since a turnbuckle with no bearing was used in place of the upper link's hydraulic actuator, there is a large amount of friction in the pin joint causing the joint to exhibit some characteristics of a clamped end condition. Using the finite element method, pin-pin, clamped-pin, and clamped-clamped boundary conditions were used for the actuator link. The resulting natural frequencies were 30.1, 46, and 64 Hz, respectively. From this, it is concluded that the difference between the measured natural frequencies and the predicted one is due to the friction in the joints of the actuator link.

In the fourth system mode, there is a 6 Hz discrepancy between the measured natural frequency and the frequency predicted by the finite element method. In Fig. 5d, it can be seen that the fourth mode also involves the movement of the joint at point C on Fig. 4. This discrepancy is attributed to the same effects that cause the discrepancy in the third mode. Also, note that the 54.37 Hz fourth mode is not predicted accurately by the assumed modes method. The reason for this is that the assumed modes method ignores the movement of the lower part of the lower link. Since the fourth mode's movement is dominated by the bending of the lower link, the assumed mode method cannot predict this mode accurately. When the finite element method model 1 was adjusted to reflect the same assumptions used in the assumed modes model, the results of these two theoretical methods agreed well. See Table 1. The assumed modes model has been improved to represent these effects but with much increased complexity.

The fourth system mode was originally overlooked by the assumed modes method because of the assumption that the point, C, on Fig. 4 had no displacement and that the hydraulic actuator and Link 1 were rigid. The fact that one of the system's modes was completely missed by the assumed modes method shows the importance of verifying theoretical results with experiments. The effect of the fourth system may be small in terms of displacement, but its effect is larger than that made by the fifth mode and may affect the control stability.

The fifth system mode, Fig. 5e, shows that the vibration of the manipulator is dominated by the second bending mode of the upper beam. This mode is predicted by both the theoretical methods and corresponds well with the experimental results.

The agreement between the three methods of analysis is substantiated by the the similar mode shapes found. There is some discrepancy in phase between the measured mode shape and the shape predicted by the finite element model in the fourth and fifth system modes. This was perhaps a result of the small magnitude of the signal at the higher frequencies and the fact that the shaker was located at only one place on the structure. Fig. 4 shows the normalized mode shapes of the structure. The displacement of the endpoint of the upper link is of the same order of magnitude for both the first and second modes of vibration. The third, fourth, and fifth mode's effect on the endpoint of the upper link are two orders of magnitude smaller than the effect of the first two modes. Therefore, the control of the first two modes of the system should be of primary concern to the designer.

Because this manipulator is a less than ideal structure, several obstacles were encountered during the experimental analysis which made getting clear information about the true system natural frequencies difficult. Chief among these were the flexibility of

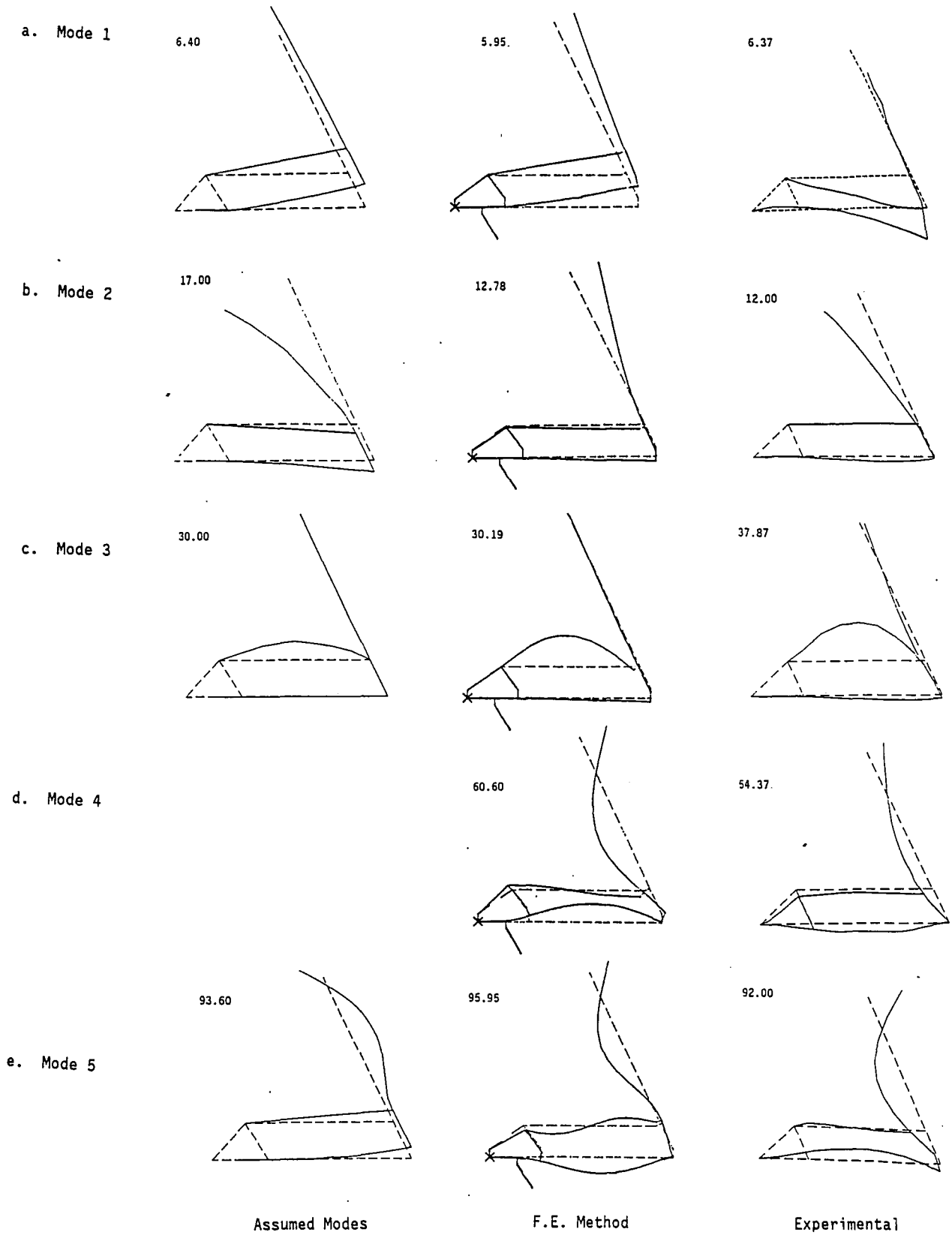

Comparison of Mode Shapes (frequency in Hz)
Fig. 5

the base and the out-of-plane vibrations. Firstly, the base structure itself was found to have a natural frequency at 30 Hz. See Figure 6. Since the theoretical results predicted a system mode at 30 Hz, it was unclear which frequency was associated with the vibration of the links. This problem was found by adding mass to the base and observing which peak on the frequency response moved and then eliminated by stiffening the base structure with steel plates.

The second problem was separating the true system in-plane modes from the out-of-plane system modes. It was here that the comparison of the experimental results with the theoretically predicted modes was very useful. The first three system modes were easily measured and were clearly separated on the frequency response plots. See Figure 7. The fourth and fifth modes, however, were obscured by the out-of-plane vibrations. The fourth mode was originally neglected due to its small magnitude. By comparison with the finite element method, the fourth mode was clearly shown to be dominated by the vibration of the lower link and that there was an out-of-plane system mode at a slightly higher frequency. Subsequent measurements confirmed both the 54.37 Hz in-plane mode and an out-of-plane mode at 63 Hz. Without the theoretical predictions of the natural frequencies and mode shapes, it would have been very time consuming to find the higher frequency mode shapes, especially since the manipulator being examined here has a number of out-of-plane frequencies that are nearly the same frequency and magnitude as the in-plane vibrations.

IV. SUMMARY AND FUTURE WORK

All the methods discussed in this paper have merit. They are particularly powerful when used in conjunction. The ability to look for system modes that are predicted by either of the theoretical methods allows much faster determination of the system mode shapes and natural frequencies by allowing the examiner to narrow his focus. When there were discrepancies between the experimental results and the theoretical, it was found that there were logical reasons for the differences. For example, the finite element method had significant differences with the experimental results at the beginning of the experiment due to the coarseness of the finite elements model. As more detail was added to the F.E. model, more agreement with the experiment was obtained. Therefore, the finite element method is an excellent tool for explaining the differences between experimental and analytical results.

The assumed modes method must use a particular set of boundary conditions in order to accurately model the manipulator. The experimental results help to determine the proper boundary conditions whereby the model can be adjusted. Also, the experimental results can indicate when the assumed modes model has included sufficient detail. The fourth mode was not predicted by the assumed modes method because the effect of the flexible lower beam on link 1 was ignored. Using the results of these three modeling techniques together, structures can be modeled quickly and accurately and with great confidence.

In addition to testing the accuracy in modeling this particular arm, the general validity of the assumed modes model of a flexible multi-joint arm with a closed loop kinematic chain is under evaluation. The significance of this model is its theoretical validity for large motions and high speeds.

Further experiments are planned to verify the large motion aspects of this model.

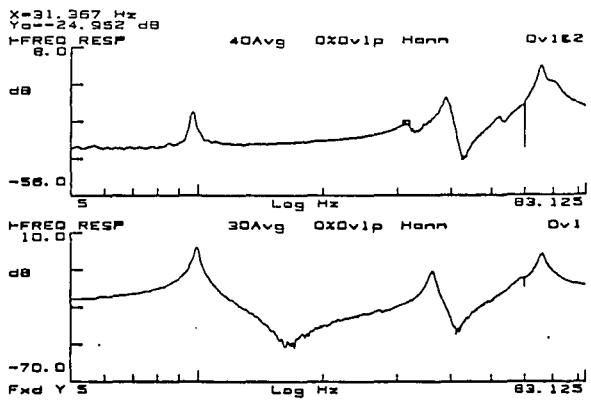

Typical Frequency Response Plot
a. before base was stiffened
b. after base was stiffened
Fig. 6

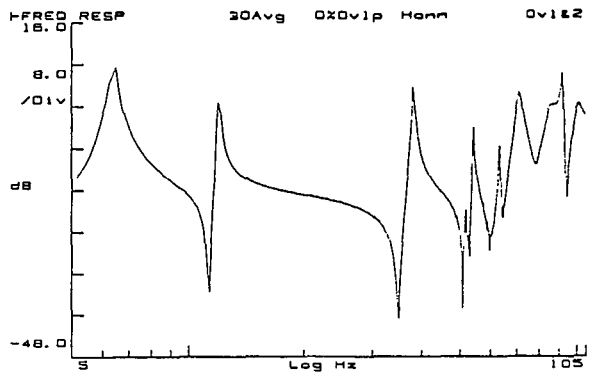

Typical Frequency Response Plot
Lower Link
Fig. 7

ACKNOWLEDGEMENTS

The authors wish to acknowledge the early experimental and modeling contributions of Dr. Ya-Chien Chung, of the National Taiwan University, while a visiting scholar at the Georgia Institute of Technology. This work was partially supported through the Computer Integrated Manufacturing Systems (CIMS) and through Grant # NAG-1-623 of the National Aeronautics and Space Administration.

BIBLIOGRAPHY

1. Wilson, Thomas R., "The Design and Construction of a Flexible Manipulator," MS Thesis, Georgia Institute of Technology, March 1986.

2. SMP Reference Manual, Inference Corporation, 1983

3. SUPERTAB User's Guide, Structural Dynamics Research Corp., 1986

4. Shabana, A.A., "Dynamics of inertia-variant flexible systems using experimentally identified parameters" Journal of Mechanisms, Transmissions, and Automation in Design, Vol. 108, pp. 358-366, 1986.

5. Laura, P.A.A., Pombo, J.L., and Susemihl, E.A., "A note on the vibration of a clamped free beam with a mass at the free end" Journal of Sound and Vibration, Vol 37, No. 2, pp. 161-168, 1974.

6. Blèvins, R.D., "Formulas for natural frequency and mode shape" Van Nostrand Reinhold, 1979.

7. Hastings, Gordon G., John F. Dorsey, Wayne J. Book, "Application of Balanced Realizations to Estimate Model Order Requirements for Flexible Manipulators," Submitted to ASME WAM, Boston, MA, 1987.

8. Ewins, D.J., "Modal Testing: Theory and Practice," Reasearch Studies Press; New York: Wiley, 1984.

9. "Application Note 243-3," Hewlett-Packard Co., Palo Alto, CA, May 1986.

10. "Application Note 243," Hewlett-Packard Co., Palo Alto, CA, Feb. 1985.

11. Operating Instructions for H-P Model 3562A Dynamic Signal Analyzer, Hewlett-Packard Co., Palo Alto, CA, 1985.

12. "Model Solution and Optimization," Structural Dynamics Research Corp., 1986.